



Block Copolymers Featuring Highly Photostable Photoacids Based on Vinylnaphthol: Synthesis and Self-Assembly

Felix Wendler, Jessica C. Tom, Maria Sittig, Philip Biehl, Benjamin Dietzek, and Felix H. Schacher*

The synthesis of a photoresponsive amphiphilic diblock quarterpolymer containing 5-vinyl-1-naphthol (VN) as a photostable photoacidic comonomer is presented. The preparation is realized via a sequential reversible addition fragmentation chain transfer (RAFT) polymerization starting from a nona(ethylene glycol) methyl ether methacrylate (MEO₉MA/"O") hydrophilic block, which is then used as a macro-RAFT agent in the terpolymerization of styrene (S), 2-vinylpyridine (2VP), and TBS-protected VN (*t*VN). The terpolymerization proceeds in a controlled fashion and two diblock quarterpolymers, P(O_m)-*b*-P(S_x-*co*-2VP_y-*co*-VN_z), with varying functional comonomer compositions are prepared. These diblock quarterpolymers form spherical core-corona micelles in aqueous media according to dynamic light scattering (DLS) and cryogenic transmission electron microscopy (cryo-TEM). Upon irradiation, the photoacids within the micellar core experience a drastic increase in acidity causing a proton transfer from the photoacid to neighboring 2VP units. As a result, the hydrophilic/hydrophobic balance of the entire assembly is shifted, and the encapsulated cargo is released.

Microphase separation of amphiphilic block copolymers (BCPs) under bulk conditions and in selective solvents is a remarkable phenomenon that has been extensively studied owing to the broad variety of nanostructures formed.^[1] In particular, the

preparation of micelles remains of high interest in biomedicine, e.g., as drug delivery systems.^[2] One approach toward achieving controlled drug delivery is the design of so-called stimuli-responsive materials, which by definition are capable of undergoing conformational and/or chemical changes upon an external (temperature, magnetic fields, or light) or an internal (pH and redox) trigger.^[3] BCPs with stimuli-responsive functionalities, which can be triggered via pH or temperature, have received significant attention in this regard.^[4] Photoresponsive polymers have also been comprehensively investigated in recent years,^[5] since the first examples of irreversible (i.e., photocleavage) and reversible (*trans*-*cis* photoisomerization) photo-triggered processes were reported in the mid-2000s.^[6] Light as an external stimulus

offers numerous advantages over other triggers; for instance, it provides both spatial and temporal control. In 2017, we introduced a novel light-responsive polymer via the incorporation of an extensively investigated excited-state photoacid, 1-naphthol,^[7] into an amphiphilic terpolymer.^[8] Excited-state photoacids are generally aromatic molecules with a protolytic group (hydroxyl functions), are usually weak acids,^[9] and have been known since the seminal work by Förster and Weller in the 1960s.^[10] Absorption of light is accompanied by a strong increase in acidity, which is associated with an excited-state acidity constant (pK_a^*) significantly lower compared to the electronic ground state (pK_a). Particularly in aqueous media, a local change in pH is anticipated. More precisely, a transfer of protons from the photoacid to the solvent occurs, and this phenomenon is known as excited-state proton transfer (ESPT).^[11] Very recently, we tested different 1-naphthol derived comonomers, and studied the effect of the linker between the chromophore and polymer backbone on the photostability and photoactivity of the respective water soluble copolymers.^[12] Among others, one particular photoacidic comonomer, i.e., 5-vinyl-1-naphthol (VN), directly connected to the polymer backbone showed excellent photostability, and the desired photoacidic properties ($\Delta pK_a \approx 8.6$, $pK_a^* \approx 0.8$). It should also be noted here, that when confined within micelles, the acidity of photoacidic moieties is typically lower than that in solution.^[13,14] However, the monomer yielding the promising photoacidic properties suffered from poor polymerizability due to steric hindrance, and potential incompatibility with the methacrylate-based comonomers used in that study.

Dr. F. Wendler, Dr. J. C. Tom, P. Biehl, Prof. F. H. Schacher
Institute of Organic and Macromolecular Chemistry (IOMC)
Friedrich Schiller University
Jena, Humboldtstrasse 10, 07743 Jena, Germany
E-mail: felix.schacher@uni-jena.de

Dr. F. Wendler, Dr. J. C. Tom, M. Sittig, P. Biehl, Prof. B. Dietzek,
Prof. F. H. Schacher
Jena Center for Soft Matter (JCSM)
Friedrich Schiller University Jena
Philosophenweg 7, 07743 Jena, Germany

M. Sittig, Prof. B. Dietzek
Institute of Physical Chemistry and Abbe Center of Photonics
Friedrich-Schiller-University Jena
Helmholtzweg 4, 07743 Jena, Germany

M. Sittig, Prof. B. Dietzek
Department Functional Interfaces
Leibniz Institute of Photonic Technology Jena
Albert-Einstein-Strasse 9, 07745 Jena, Germany

The ORCID identification number(s) for the author(s) of this article can be found under <https://doi.org/10.1002/marc.201900607>.

© 2020 The Authors. Published by WILEY-VCH Verlag GmbH & Co. KGaA, Weinheim. This is an open access article under the terms of the Creative Commons Attribution License, which permits use, distribution and reproduction in any medium, provided the original work is properly cited.

DOI: 10.1002/marc.201900607

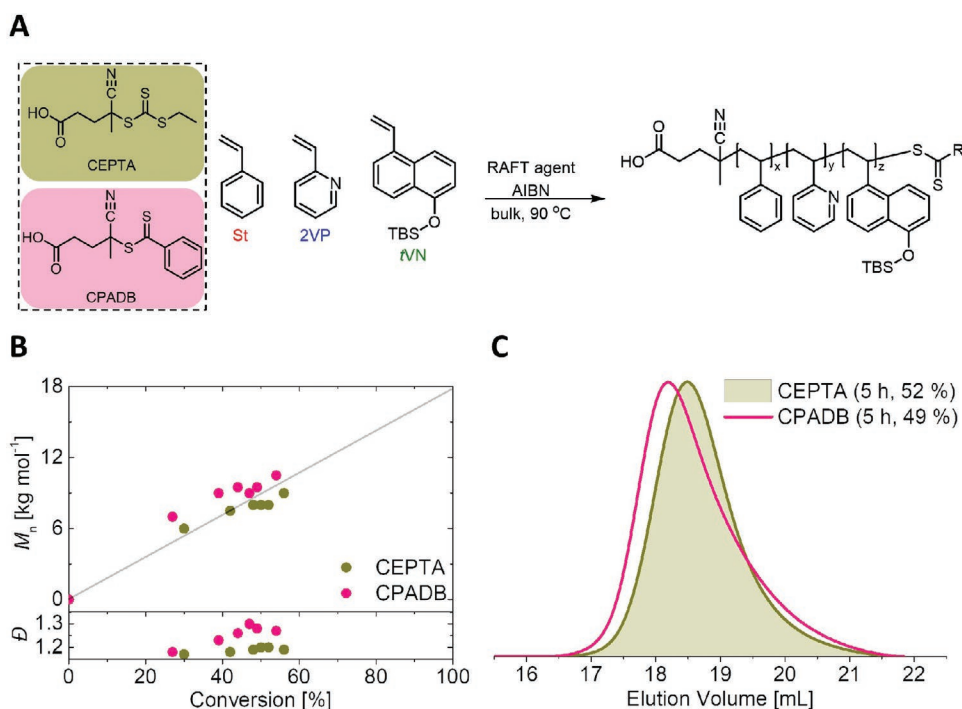


Figure 1. A) Synthetic route used to access TBS-protected amphiphilic terpolymers, P(S_x-co-2VP_y-co-tVN_z), via RAFT polymerization (AIBN, bulk, 90 °C) using either CEPTA or CPADB as the CTA. B) The corresponding M_n versus overall monomer conversion plot and C) SEC traces after 5 h.

We therefore altered our approach to access such VN-containing copolymers: we used a styrenic backbone, incorporating the photoacidic comonomer (VN) in an amphiphilic segment containing 2-vinylpyridine (2VP), a polybase, and styrene (S). In this way, light irradiation is anticipated to trigger an ESPT from the photoacid to the neighboring 2VP units. In turn, the 2VP units become protonated upon the ESPT and shift the overall hydrophilic/hydrophobic balance of the P(S_x-co-2VP_y-co-VN_z) terpolymer. The terpolymerization was conducted using the TBS-protected photoacidic comonomer, i.e., tVN, to prevent side reactions during the polymerization process, and which consequently requires subsequent deprotection. Based on previous results regarding well-defined P(S-co-2VP) copolymers via reversible addition fragmentation chain transfer (RAFT) polymerization, a dithiobenzoate-based RAFT agent, CPADB, was chosen.^[15] In addition to that RAFT agent we included 4-cyano-4-[[[dodecylthio]carbonothioyl]thio]pentanoic acid (CEPTA), a trithiocarbonate, which generally affords better control over styrenic-based monomers compared to CPADB (Figure 1C).^[16]

Furthermore, CEPTA is compatible with methacrylates as well, which is particularly interesting in terms of introducing a second hydrophilic block for the formation of block copolymer micelles. The terpolymerization of tVN, 2VP and S was studied using a feed ratio of [monomer]:[CTA]:[I] = 125:1:0.25, with a [S]:[2VP]:[tVN] ratio of 0.6:0.2:0.2. As often reported for the radical polymerization of styrenes, bulk conditions and high temperatures were applied (90 °C, AIBN as thermal initiator). As seen from Figure 1B, an increasing M_n with overall monomer conversion in accordance to theory was found, indicating the terpolymerization proceeds in a controlled manner independent of the RAFT agent used, CEPTA or CPADB. However, slightly higher molecular weights are observed for the ter-

polymerization using CPADB with corresponding dispersities >1.2. Representative size exclusion chromatography (SEC) traces after 5 h are shown in Figure 1C, and reveal slight tailing when CPADB is used as the RAFT agent. This tailing implies chain termination is more pronounced when CPADB is used in contrast to CEPTA, which is characterized by more symmetrical molecular weight distributions and lower dispersities (≤1.2). The terpolymerization using CEPTA was therefore investigated in more detail, and the semilogarithmic plot of the respective comonomers is shown in Figure 2A, which display similar slopes over the course of the polymerization. This is a good indication that the monomers are consumed at comparable rates.

From the similar slopes observed in Figure 2A, it is reasonable to assume that each comonomer is consumed at comparable rates over the course of the polymerization, and therefore it is quite likely that the comonomers are more or less arranged randomly along the terpolymer chain. The higher conversions of 2VP compared to tVN and S are in agreement with reported reactivity ratios for radical copolymerizations of 2VP with S.^[17] Consequently, there is a slight preference to incorporate 2VP, which we have also observed previously in our group.^[15] To further evaluate this assumption, the copolymerization of S and 2VP (1:1 ratio) or S and tVN (1:1 ratio) was examined (Figure 2B). 2VP reacts more rapidly than S when copolymerized; whereas tVN and S are consumed at similar, but at significantly lower rates when copolymerized compared to S and 2VP. The lower overall monomer conversions observed in this case may result from the sterically more demanding tVN, leading to retardation of the overall copolymerization.

Regardless of these findings, terpolymers of 2VP, tVN, and S of well-defined molecular weight and low dispersities are easily accessible. This is apparent through the almost linear

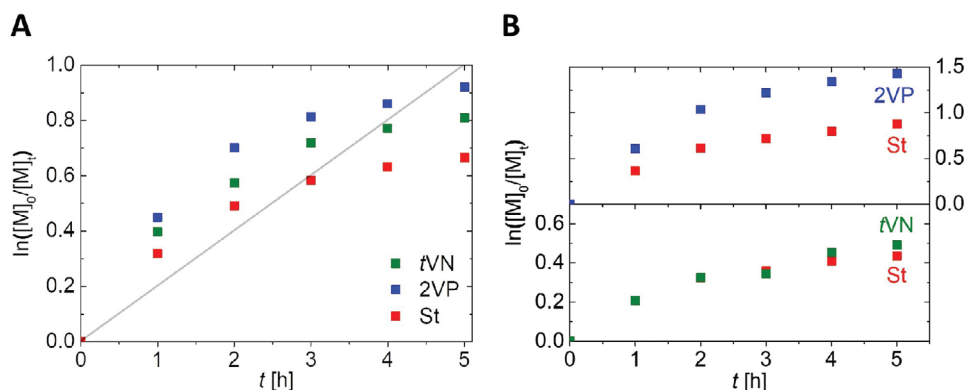


Figure 2. A) Semilogarithmic plot for the terpolymerization of tVN with S and 2VP with a [monomer]:[CEPTA] = 125:1 and B) semilogarithmic plot for the copolymerization of S with either 2VP (top) or tVN (bottom) with a [monomer]:[CEPTA] = 125:1.

semi-logarithmic plot observed within the first 3 h of copolymerization (Figure 2A), and the increasing M_n with overall monomer conversion in accordance to theory (Figure 1B). With these agreeable findings, we went on to synthesize block copolymers capable of micellization in aqueous media with a hydrophobic $P(S_x\text{-}co\text{-}2VP_y\text{-}co\text{-}VN_z)$ terpolymer block. As a hydrophilic segment, we focused on nona(ethylene glycol) methyl ether methacrylate (MEO₉MA or “O”), which is a poly(ethylene glycol) (PEG)-based building block that is readily water soluble, and which can be easily polymerized via controlled radical polymerization techniques.^[18] Moreover, the synthesis of block copolymers of MEO₉MA and styrene by RAFT has been reported using a RAFT agent similar to CEPTA.^[19] Analogous to this, the synthesis of such block copolymers was realized by considering the monomer reactivity (methacrylate > styrene) starting from a PMEO₉MA homopolymer, denoted $P(O)_n$, which was applied as a macro-RAFT agent. In contrast to the terpolymerizations using CEPTA or CPADB as RAFT agent, very low conversions (<5 %) were observed for the block extensions, which is, however, to be expected and has been reported similarly for a less sterically demanding block extension using only styrene.^[20] After using this sequential RAFT approach, a subsequent deprotection step of the TBS-protected photoacidic comonomer, tVN, was carried out to yield photoactive diblock quarterpolymers $P(O)_m\text{-}b\text{-}P(S_x\text{-}co\text{-}2VP_y\text{-}co\text{-}VN_z)$ (Figure 3A).

Since the terpolymerization of S, 2VP, and tVN was well-controlled, we performed a block extension from the $P(O)_n$ macro-RAFT agent under the same reaction conditions. The macro-RAFT agent was characterized by a molecular weight of 18 kg mol⁻¹ according to SEC analysis, and a calculated degree of polymerization (DP_n) of 45 from the monomer conversion determined using ¹H-NMR spectroscopy. This corresponds to a molar mass of 23 kg mol⁻¹. Since preliminary test reactions for the block extension of $P(O)_n$ revealed very low conversions, an excess of monomer was used in the initial feed such that the [monomer]:[macro-RAFT agent]:[I] = 500:1:0.25. The respective comonomer ratios were maintained, i.e., [S]:[2VP]:[tVN] = 0.6:0.2:0.2. After 5 h, the polymerization was terminated, and the protected diblock quarterpolymer, $P(O)_m\text{-}b\text{-}P(S_x\text{-}co\text{-}2VP_y\text{-}co\text{-}tVN_z)$ (indices depict the respective mol fraction in % as calculated from NMR spectroscopy), was separated from unreacted monomer via preparative size exclusion chromatography

(Biobeads S-X1) using THF as eluent. Preparative SEC permits the isolation of high purity block copolymers in high yields. SEC analysis of the pure protected diblock quarterpolymer showed a significant shift in elution volume (Figure 3B), characterized by a molar mass of 27 kg mol⁻¹ (PS calibration). Due to the low overall monomer conversion, we refrained from estimating the DP_n of the block copolymer; instead, ¹H-NMR spectroscopy (CD₂Cl₂) was used to determine the relative monomer composition from the $P(O)_n$ block signal at 3.4 ppm (Figure 3A), which leads to an overall DP_n of 104 for this block, and corresponding total molar mass of 38 kg mol⁻¹. Moreover, the comonomer content was calculated by integrating the characteristic ¹H-NMR signals; the protected diblock quarterpolymer composition was determined to be $P(O_{0.29})\text{-}b\text{-}P(S_{0.35}\text{-}co\text{-}2VP_{0.19}\text{-}co\text{-}tVN_{0.17})$. The results are summarized in Table 1.

An additional diblock quarterpolymer was synthesized, $P(O_{0.37})\text{-}b\text{-}P(S_{0.13}\text{-}co\text{-}2VP_{0.26}\text{-}co\text{-}tVN_{0.24})$, with a lower styrene content or higher hydrophilicity compared to $P(O_{0.29})\text{-}b\text{-}P(S_{0.35}\text{-}co\text{-}2VP_{0.19}\text{-}co\text{-}tVN_{0.17})$. In this case, a stronger photoresponse is expected under light exposure due to the higher functional comonomer content incorporated here. To obtain the final materials, $P(O_{0.29})\text{-}b\text{-}P(S_{0.35}\text{-}co\text{-}2VP_{0.19}\text{-}co\text{-}VN_{0.17})$ and $P(O_{0.37})\text{-}b\text{-}P(S_{0.13}\text{-}co\text{-}2VP_{0.26}\text{-}co\text{-}VN_{0.24})$, a deprotection step was carried out using a two-fold excess of TBAF with respect to the TBS-protected tVN repetition units in an equimolar combination with acetic acid according to a literature procedure.^[21] ¹H-NMR spectroscopy was used to characterize the deprotected diblock quarterpolymers (Figure 3C). The disappearance of the signal at 0.3 ppm corresponding to the protecting group indicates a successful deprotection. In agreement with our previous observations, an increase in molecular weight by SEC was observed (Table 1).^[8] This behavior is a consequence of stronger hydrogen bonding after deprotection due to the higher hydroxyl group concentration, and hence the deprotected polymers interact more with the SEC columns besides the predominant polymer-polymer interactions. The polymers were also subjected to preparative size exclusion chromatography (BioBeads SX-1) with THF as eluent in order to remove residual TBAF before further characterization and micellization studies were performed. The hydrophilic content of the final diblock quarterpolymers was also assessed, i.e., the mol fraction of the MEO₉MA block (abbreviated “O” in Table 1).

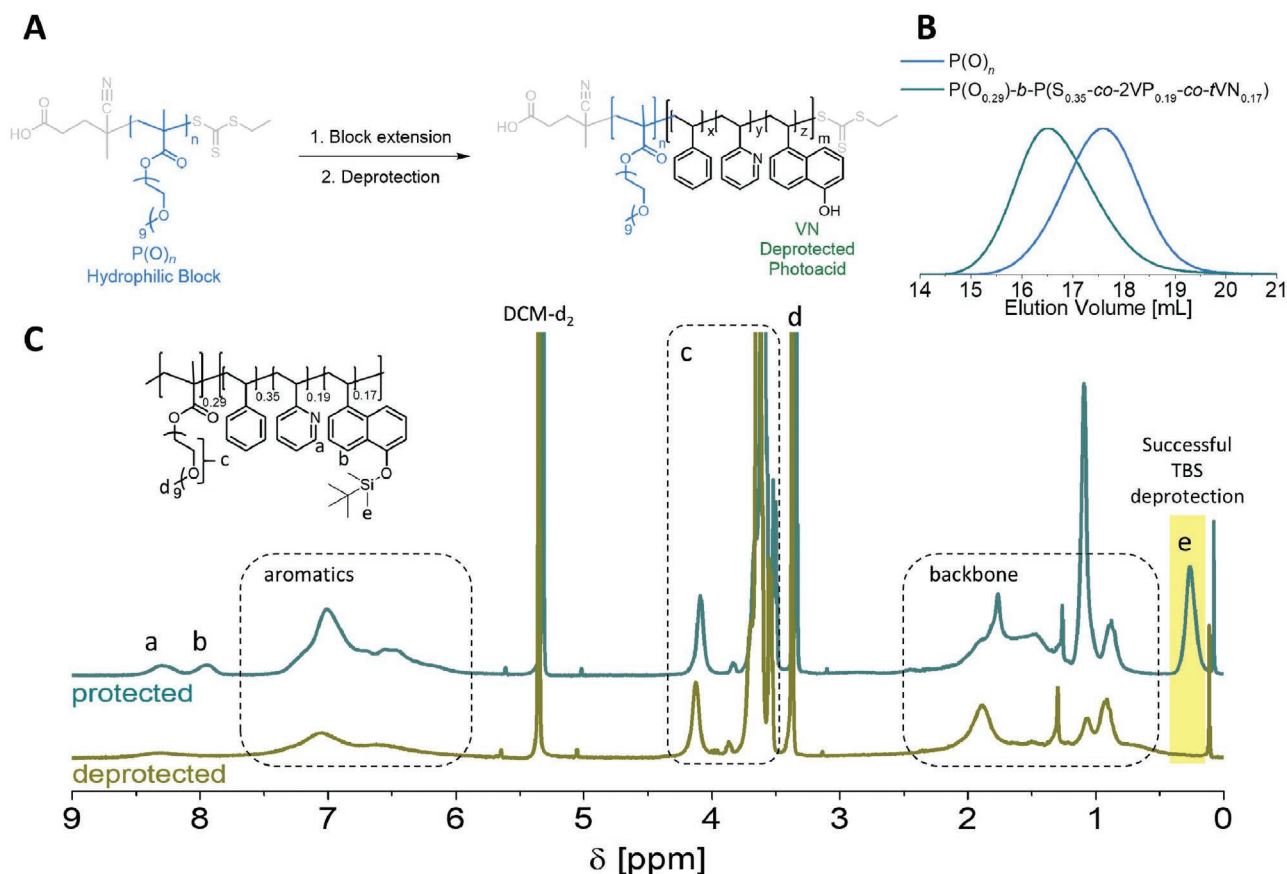


Figure 3. A) Synthetic route used to access TBS-protected amphiphilic block copolymers, $P(O_n)\text{-}b\text{-}P(S_x\text{-}co\text{-}2VP_y\text{-}co\text{-}tVN_z)$, via RAFT polymerization (AIBN, bulk, 90 °C) and subsequent deprotection (TBAF/acetic acid, THF, 0 °C). B) SEC traces showing the successful chain extension of $P(O)_n$ yielding $P(O_{0.29})\text{-}b\text{-}P(S_{0.35}\text{-}co\text{-}2VP_{0.19}\text{-}co\text{-}tVN_{0.17})$ and C) representative $^1\text{H-NMR}$ spectra showing the successful deprotection of TBS-protected $P(O_{0.29})\text{-}b\text{-}P(S_{0.35}\text{-}co\text{-}2VP_{0.19}\text{-}co\text{-}tVN_{0.17})$.

After preparing the desired photoacid-containing diblock quarterpolymers, $P(O_{0.29})\text{-}b\text{-}P(S_{0.35}\text{-}co\text{-}2VP_{0.19}\text{-}co\text{-}tVN_{0.17})$ and $P(O_{0.37})\text{-}b\text{-}P(S_{0.13}\text{-}co\text{-}2VP_{0.26}\text{-}co\text{-}tVN_{0.24})$, we investigated their self-assembly in water as a selective solvent. This was achieved by first dissolving the respective diblock quarterpolymers in THF as a nonselective solvent, followed by adding the solution dropwise into micropure water under vigorous stirring. The assemblies, which presumably consist of a $P(S_x\text{-}co\text{-}2VP_y\text{-}co\text{-}tVN_z)$ core and a $P(O)_n$ corona, were

realized by stirring the mixtures for an additional 24 h to allow the volatile THF to evaporate. Dynamic light scattering (DLS) and cryogenic transmission electron microscopy (cryo-TEM) were then used to investigate the size and structure of the formed assemblies (Table 1 and Figure 4). According to DLS measurements, the number-weighted particle size for both diblock quarterpolymers, $P(O_{0.29})\text{-}b\text{-}P(S_{0.35}\text{-}co\text{-}2VP_{0.19}\text{-}co\text{-}tVN_{0.17})$ and $P(O_{0.37})\text{-}b\text{-}P(S_{0.13}\text{-}co\text{-}2VP_{0.26}\text{-}co\text{-}tVN_{0.24})$, are within 5–10 nm (Figure 4A).

Table 1. Characterization of the macro-RAFT agent, the protected and deprotected block copolymers (SEC, NMR), and the prepared micellar solutions (DLS).

Sample	$M_{n,SEC}^a$ [kg mol ⁻¹]	\bar{D}^a	Conv ^b [%]	DP _n (block)	M_n [kg mol ⁻¹]	O ^c [wt%]	$\langle R_h \rangle_{n,app}^d$ [nm]
$P(O)_n$	18	1.23	57	45 ^e	23	–	–
$P(O_{0.29})\text{-}b\text{-}P(S_{0.35}\text{-}co\text{-}2VP_{0.19}\text{-}co\text{-}tVN_{0.17})$	27	1.41	4	104 ^d	38	29.0	–
$P(O_{0.37})\text{-}b\text{-}P(S_{0.13}\text{-}co\text{-}2VP_{0.26}\text{-}co\text{-}tVN_{0.24})$	30	1.31	–*	70 ^f	35	36.9	–
$P(O_{0.29})\text{-}b\text{-}P(S_{0.35}\text{-}co\text{-}2VP_{0.19}\text{-}co\text{-}tVN_{0.17})$	34	1.39	–	–	–	–	6.3 ± 1.9
$P(O_{0.37})\text{-}b\text{-}P(S_{0.13}\text{-}co\text{-}2VP_{0.26}\text{-}co\text{-}tVN_{0.24})$	39.5	1.31	–	–	–	–	9.6 ± 0.5

^a) Determined by SEC (DMAc/LiCl) (PS calibration); ^b) $^1\text{H-NMR}$ (300 MHz, CDCl₃); ^c) Mol fraction of the MEO₉MA block (abbreviated "O") or hydrophilic content determined using $^1\text{H-NMR}$ (300 MHz, CD₂Cl₂); ^d) Determined by DLS, *no conversion could be determined in this case. The indices of the polymers depict the composition determined via $^1\text{H-NMR}$ (300 MHz, CD₂Cl₂) or in case of $P(O)_n$ it depicts the DP which could be estimated from the conversion; ^e) Determined from the conversion; ^f) Determined from $^1\text{H-NMR}$ (300 MHz, CD₂Cl₂) using the $P(O)_n$ signal at 3.4 ppm as a reference.

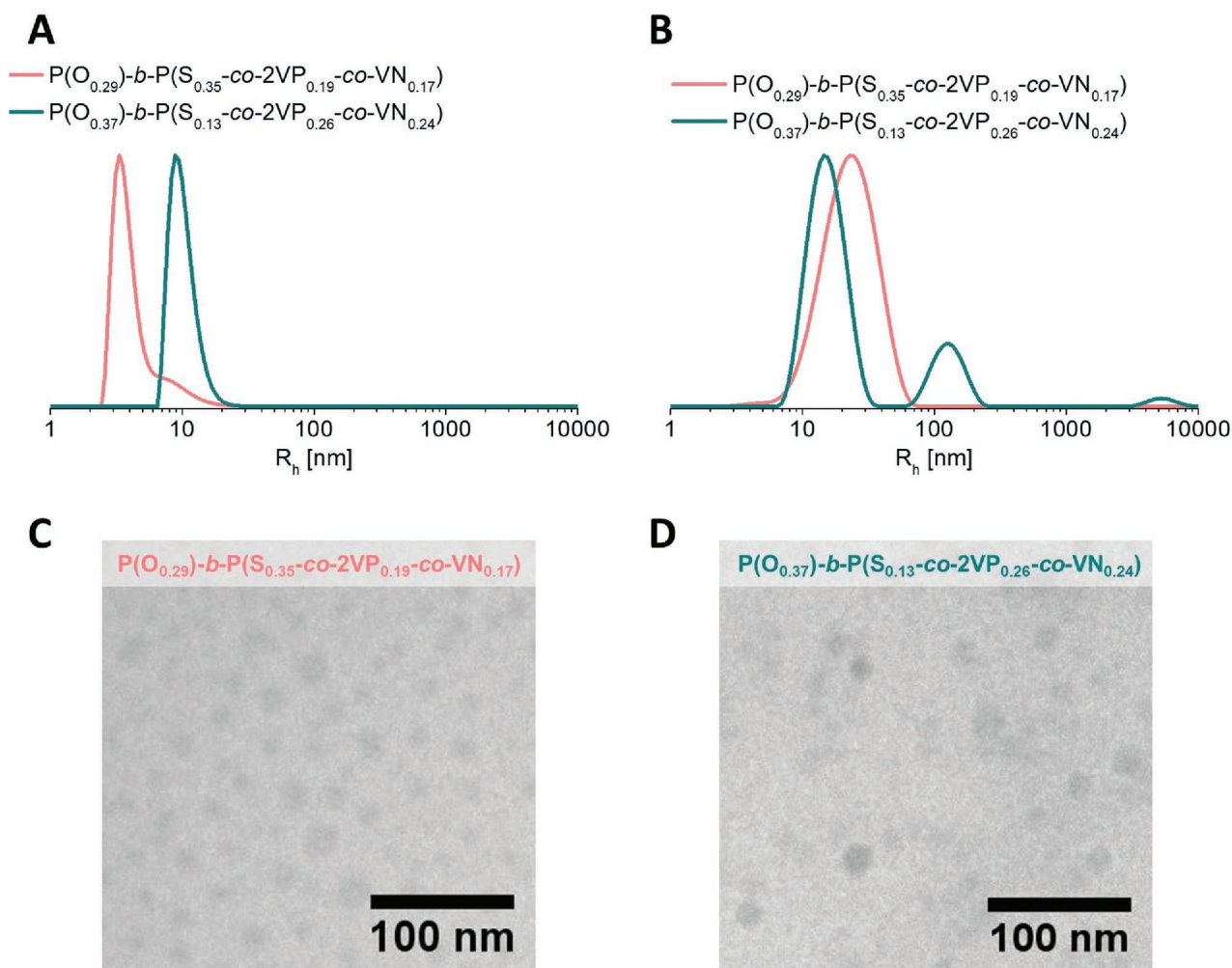


Figure 4. A) Number-weighted hydrodynamic radius of the diblock quarterpolymer micelles and B) intensity-weighted hydrodynamic radius of the prepared diblock quarterpolymer micelles ($c = 1 \text{ mg mL}^{-1}$) and their corresponding cryo-TEM images: C) $\text{P}(\text{O}_{0.29})\text{-}b\text{-P}(\text{S}_{0.35}\text{-co-}2\text{VP}_{0.19}\text{-co-VN}_{0.17})$ and D) $\text{P}(\text{O}_{0.37})\text{-}b\text{-P}(\text{S}_{0.13}\text{-co-}2\text{VP}_{0.26}\text{-co-VN}_{0.24})$.

The intensity-weighted hydrodynamic radii show broader distributions with slightly increased radii of 23 nm ($\text{P}(\text{O}_{0.29})\text{-}b\text{-P}(\text{S}_{0.35}\text{-co-}2\text{VP}_{0.19}\text{-co-VN}_{0.17})$) and 15 nm ($\text{P}(\text{O}_{0.37})\text{-}b\text{-P}(\text{S}_{0.13}\text{-co-}2\text{VP}_{0.26}\text{-co-VN}_{0.24})$) (Figure 4B). Larger aggregates ($>100 \text{ nm}$) are also observed in the latter case. Both observations can be explained by the fact that the scattering intensity is proportional to the 6th power of the particle radius, which leads to an apparent discrimination of smaller particles, even though they may represent the major fraction. Cryo-TEM micrographs reveal similar results with diameters ranging from 10 nm up to 30 nm, and which are fairly spherical in shape. This relatively broad distribution may arise due to a higher degree of intermolecular hydrogen bonding interactions for the $\text{P}(\text{O}_{0.37})\text{-}b\text{-P}(\text{S}_{0.13}\text{-co-}2\text{VP}_{0.26}\text{-co-VN}_{0.24})$ micelles compared to the $\text{P}(\text{O}_{0.29})\text{-}b\text{-P}(\text{S}_{0.35}\text{-co-}2\text{VP}_{0.19}\text{-co-VN}_{0.17})$ micelles, which presumably leads to the formation of these larger aggregates. In the literature, strong interactions between pyridines and phenols have been reported,^[22–25] which likewise may explain the formation of larger aggregates or nonuniform micelles during the self-assembly process of the systems reported here.

Upon exposure to UV light, the photoacid becomes activated and experiences a strong shift in acidity. We anticipate this to result in an ESPT from the photoacid to neighboring 2VP units (Figure 5A). The presence of charged groups within the micellar core is then expected to shift the overall hydrophilic/hydrophobic balance of the entire diblock quarterpolymer. This will in turn lead to swelling and possibly dissolution of the respective micelles into unimers. The photoactivation, and possible swelling and/or disruption of the formed micelles, is further supported by reproducible changes observed by dynamic light scattering with irradiation at 365 nm for 60 min (Figure S4, Supporting Information).

As a proof of concept for drug delivery applications, we investigated whether these diblock quarterpolymer micelles are capable of releasing encapsulated cargo triggered by UV light (irradiation at 365 nm). As a model hydrophobic guest molecule, we considered Nile Red (NR), which was loaded into the micelles via coprecipitation. The potential release of Nile Red was monitored by fluorescence emission spectroscopy at an excitation wavelength of 510 nm, a wavelength at

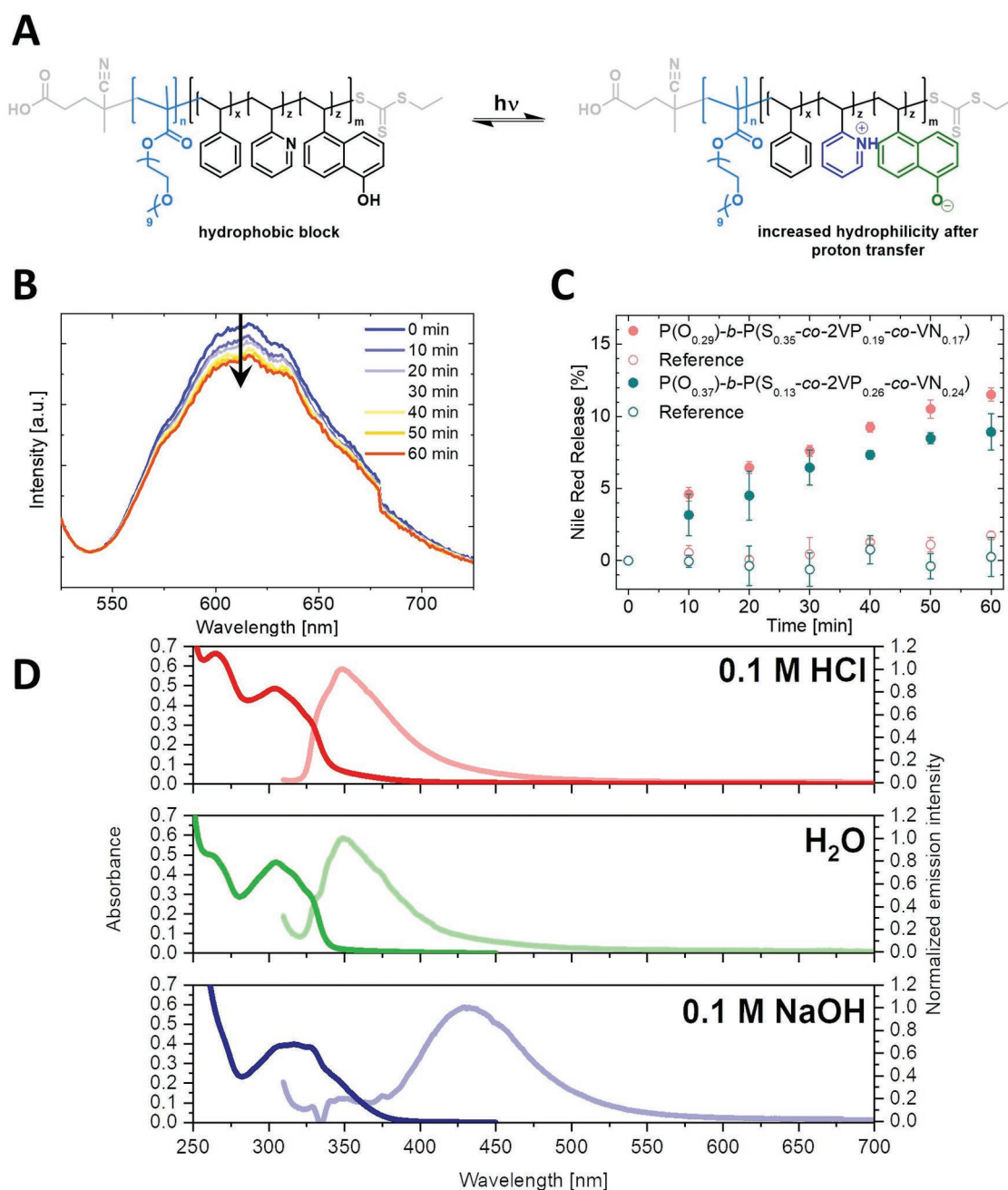


Figure 5. A) Depiction of the reversible light-mediated proton transfer resulting in a shift in the overall hydrophilic/hydrophobic balance of the P(O_m)-b-P(S_x-co-2VP_y-co-VN_z) diblock quarterpolymer. B) Exemplary fluorescence emission spectra showing the reduction in Nile Red fluorescence with increasing irradiation time (365 nm) and C) the calculated amount of Nile Red released from the diblock quarterpolymer micelles of P(O_{0.29})-b-P(S_{0.35}-co-2VP_{0.19}-co-VN_{0.17}) and P(O_{0.37})-b-P(S_{0.13}-co-2VP_{0.26}-co-VN_{0.24}) with (closed circles) and without (open circles) irradiation. D) UV/vis absorption and emission (light colored) spectra of P(O_{0.29})-b-P(S_{0.35}-co-2VP_{0.19}-co-VN_{0.17}) micelles in aqueous media: 0.1 M HCl (red, pH 1), H₂O (green, pH 6), and 0.1 M NaOH (blue, pH 13).

which the photoacid does not absorb light. Upon irradiation at 365 nm, the emission intensity of NR at ≈ 615 nm decreases (Figure 5B). This may indicate that the NR is released from the micelles to the polar water phase, where its emission is effectively quenched. However, it should be noted that the fluorescence quantum yield of NR does not only depend on the environment or polarity of the solvent, but also on the

concentration of NR, the concentration of micelles, and the aggregation number of the respective micelle.^[26] Consequently, a reduction in the NR emission does not unambiguously prove the release of NR from the polymer micelles, but may result from a number of factors, e.g., increased polarity of the core due to photoactivation and swelling. However, the decrease in NR fluorescence upon increasing irradiation time

proves that the micelles do indeed exhibit photoresponsive behavior.

If we assume that the reduction in the NR emission arises exclusively from successful cargo release through photodriven swelling or conformational changes, the extent of NR release can be estimated from the fluorescence emission intensity at ≈ 615 nm using Equation S1 (Figure 5C). Employing this assumption, ≈ 10 % of the loaded Nile Red is released within 60 min upon irradiation at 365 nm for both $P(O_{0.37})\text{-}b\text{-}P(S_{0.13}\text{-}co\text{-}2VP_{0.26}\text{-}co\text{-}VN_{0.24})$ and $P(O_{0.29})\text{-}b\text{-}P(S_{0.35}\text{-}co\text{-}2VP_{0.19}\text{-}co\text{-}VN_{0.17})$ diblock quarterpolymer micelles. This is lower than for the previously reported systems comprising MMA and DMAEMA as comonomers of up to 30% in 60 min.^[8,12,27] The significant decrease in release kinetics in the current system likely arises from confinement effects: the reduced photoacidity of the VN moiety hinders the formation of charged species in a confined space.^[13] This is further exacerbated by the increased hydrophobicity of the styrene-based core compared to the previously used methacrylate-based system, and slower dynamics associated with higher T_g polymer segments within the micellar core. Moreover, the T_g is expected to be increased (in the range of 162–173 °C as has been reported for bulk materials) caused by the strong interactions between pyridines and phenols.^[22–25] This effect was found to be less pronounced in the case of similar systems possessing DMAEMA moieties instead of pyridines; here only a moderate increase was reported in the literature (113–135 °C),^[28] and this may explain the deviating observations compared to our previous reports.

Aqueous solutions of the respective VN-containing BCP micelles were investigated by steady-state absorption and emission spectroscopy. Exemplary absorption and emission spectra for the $P(O_{0.29})\text{-}b\text{-}P(S_{0.35}\text{-}co\text{-}2VP_{0.19}\text{-}co\text{-}VN_{0.17})$ micelles at select pH values, i.e., in 0.1 M HCl (pH 1), H₂O (pH 6), and 0.1 M NaOH (pH 13), are shown in Figure 5D. The protonated form absorbs at around 300 nm, whereas the corresponding 1-naphtholate exhibits a red-shifted absorption centered at around 340 nm. The respective emission maxima of 1-naphthol and 1-naphtholate species are located at 350 and 430 nm, respectively. All BCP micelles exhibit the emission of protonated 1-naphthol exclusively in water (Figure S6 in the Supporting Information for more details). This observation suggests the VN moieties within the micellar core are not sufficiently solvated to mediate an ESPT under these conditions. This result is contrary to the results obtained in the NR release studies (Figure 5C), which indicate the BCP micelles undergo a light-mediated release upon irradiation at 365 nm. However, in view of potentially higher T_g values caused by the interpolymer complex formation between 1-naphthol and pyridine,^[22] this observation may be explained by the resultant glassy nature of the core that suppresses any migration of water molecules toward the photoacid moieties. Given the uncertainties in the quantification of the cargo release and its direct correlation with micelle swelling, we suggest that only a small fraction of the VN units can be deprotonated after excitation, and therefore the change in the hydrophobic/hydrophilic balance is limited. This may result in the observed lower release of NR compared to our previous studies. However, the exact mechanism of the light-mediated release for this particular system, especially in comparison to other reported photoacids, needs to be further investigated.

In summary, we presented the synthesis of well-defined and light-responsive terpolymers containing tVN via RAFT, a photostable photoacidic comonomer in combination with styrene and 2-vinylpyridine. After studying the terpolymerization using two different chain transfer agents, we prepared two amphiphilic block copolymers under optimized conditions with varying amounts of photoacid via a block extension from a hydrophilic PMEO₃MA macro-RAFT agent capable of forming spherical micelles. Their micellization in water was investigated; and subsequently, their light-triggered release of an encapsulated model cargo was demonstrated. We see great potential for these materials in controlled drug delivery and other fields where spatial and temporal control over macromolecular conformation and net charge or charge density is an advantage.

Supporting Information

Supporting Information is available from the Wiley Online Library or from the author.

Acknowledgements

This research was supported by the DFG within the collaborative research centre SFB 1278 POLYTARGET (project number 316213987), project A03. The authors thank Philip Biehl for cryo-TEM investigations. The cryo-TEM/TEM facilities of the Jena Center for Soft Matter (JCSM) were established with a grant from the German Research Council (DFG) and the European Funds for Regional Development (EFRE).

Conflict of Interest

The authors declare no conflict of interest.

Keywords

amphiphilic block copolymers, light-responsive materials, photoacids, RAFT, self-assembly

Received: November 18, 2019

Revised: January 8, 2020

Published online: February 9, 2020

- [1] a) F. S. Bates, G. H. Fredrickson, *Annu. Rev. Phys. Chem.* **1990**, *41*, 525; b) F. S. Bates, G. H. Fredrickson, *Phys. Today* **1999**, *52*, 32; c) G. Riess, *Prog. Polym. Sci.* **2003**, *28*, 1107; d) Y. Mai, A. Eisenberg, *Chem. Soc. Rev.* **2012**, *41*, 5969; e) F. H. Schacher, P. A. Rupar, I. Manners, *Angew. Chem., Int. Ed.* **2012**, *51*, 7898; f) C. M. Bates, F. S. Bates, *Macromolecules* **2017**, *50*, 3; g) U. Tritschler, S. Pearce, J. Gwyther, G. R. Whittell, I. Manners, *Macromolecules* **2017**, *50*, 3439.
- [2] a) C. Allen, D. Maysinger, A. Eisenberg, *Colloids Surf., B* **1999**, *16*, 3; b) K. Kataoka, A. Harada, Y. Nagasaki, *Adv. Drug Delivery Rev.* **2001**, *47*, 113; c) A. Rösler, G. W.M. Vandermeulen, H.-A. Klok, *Adv. Drug Delivery Rev.* **2001**, *53*, 95; d) G. Gaucher, M.-H. Dufresne, V. P. Sant, N. Kang, D. Maysinger, J.-C. Leroux, *J. Controlled Release* **2005**, *109*, 169; e) A. Blanz, S. P. Armes, A. J. Ryan, *Macromol.*



- Rapid Commun.* **2009**, *30*, 267; f) H. Cabral, K. Miyata, K. Osada, K. Kataoka, *Chem. Rev.* **2018**, *118*, 6844.
- [3] M. A. C. Stuart, W. T. S. Huck, J. Genzer, M. Müller, C. Ober, M. Stamm, G. B. Sukhorukov, I. Szleifer, V. V. Tsukruk, M. Urban, F. Winnik, S. Zauscher, I. Luzinov, S. Minko, *Nat. Mater.* **2010**, *9*, 101.
- [4] a) V. P. Torchilin, *Pharm. Res.* **2006**, *24*, 1; b) N. Rapoport, *Prog. Polym. Sci.* **2007**, *32*, 962; c) M.-H. Li, P. Keller, *Soft Matter* **2009**, *5*, 927; d) O. Onaca, R. Enea, D. W. Hughes, W. Meier, *Macromol. Biosci.* **2009**, *9*, 129; e) Z. Ge, S. Liu, *Chem. Soc. Rev.* **2013**, *42*, 7289.
- [5] a) Y. Zhao, *Chem. Rec.* **2007**, *7*, 286; b) J.-F. Gohy, Y. Zhao, *Chem. Soc. Rev.* **2013**, *42*, 7117; c) Y. Zhao, *Macromolecules* **2012**, *45*, 3647; d) J.-M. Schumers, C.-A. Fustin, J.-F. Gohy, *Macromol. Rapid Commun.* **2010**, *31*, 1588; e) O. Grimm, F. Wendler, H. F. Schacher, *Polymers* **2017**, *9*, 396.
- [6] a) J. Jiang, X. Tong, Y. Zhao, *J. Am. Chem. Soc.* **2005**, *127*, 8290; b) G. Wang, X. Tong, Y. Zhao, *Macromolecules* **2004**, *37*, 8911.
- [7] E. Pines, "UV-Visible Spectra and Photoacidity of Phenols, Naphthols and Pyrenols", in *The Chemistry of Phenols*, John Wiley & Sons, Ltd, Chichester, UK **2003**, p. 491.
- [8] F. Wendler, K. R. A. Schneider, B. Dietzek, F. H. Schacher, *Polym. Chem.* **2017**, *8*, 2959.
- [9] J. F. Ireland, P. A. H. Wyatt, *Advances in Physical Organic Chemistry, Acid-Base Properties of Electronically Excited States of Organic Molecules*, Vol. 12, Elsevier, Amsterdam **1976**, p. 131.
- [10] a) T. Förster, *Sci. Nat.* **1949**, *36*, 186; b) T. Förster, *Z. Elektrochem. Angew. Phys. Chem.* **1950**, *54*, 42; c) A. Weller, *Z. Elektrochem. Angew. Phys. Chem.* **1952**, *56*, 662; d) A. Weller, *Z. Elektrochem. Angew. Phys. Chem.* **1954**, *58*, 849; e) A. Weller, *J. Phys. Chem.* **1958**, *17*, 224; f) A. Weller, *Progress in Reaction Kinetics*, Vol. 1, 1st ed, Pergamon Press, New York **1961**, p. 187.
- [11] a) M. Gutman, E. Nachliel, *Biochim. Biophys. Acta, – Bioenerg.* **1990**, *1015*, 391; b) L. G. Arnaut, S. J. Formosinho, *J. Photochem. Photobiol., A* **1993**, *75*, 1; c) L. M. Tolbert, K. M. Solntsev, *Acc. Chem. Res.* **2002**, *35*, 19; d) N. Agmon, *J. Phys. Chem. A* **2005**, *109*, 13.
- [12] F. Wendler, M. Sittig, J. C. Tom, B. Dietzek, F. H. Schacher, *Chem. Eur. J.* **2020**, <https://doi.org/10.1002/chem.201903819>.
- [13] C. D. Sanborn, J. V. Chacko, M. Digman, S. Ardo, *Chem* **2019**, *5*, 1648.
- [14] a) W. White, C. D. Sanborn, R. S. Reiter, D. M. Fabian, S. Ardo, *J. Am. Chem. Soc.* **2017**, *139*, 11726; b) W. White, C. D. Sanborn, D. M. Fabian, *Joule* **2018**, *2*, 94; c) M. Gutman, D. Huppert, *J. Biochem. Biophys. Methods* **1979**, *1*, 9; d) M. Gutman, D. Huppert, E. Pines, *J. Am. Chem. Soc.* **1981**, *103*, 3709.
- [15] M. Billing, J. K. Elter, F. H. Schacher, *Polymer* **2016**, *104*, 40.
- [16] a) G. Moad, E. Rizzardo, S. H. Thang, *Polymer* **2008**, *49*, 1079; b) S. Perrier, *Macromolecules* **2017**, *50*, 7433.
- [17] a) T. Tamikado, *J. Polym. Sci.* **1960**, *43*, 489; b) J. Lokaj, P. Holler, *J. Appl. Polym. Sci.* **2001**, *80*, 2024.
- [18] J.-F. Lutz, *J. Polym. J. Polym. Sci., Part A: Polym. Chem.* **2008**, *46*, 3459.
- [19] W. Zhao, G. Gody, S. Dong, P. B. Zetterlund, S. Perrier, *Polym. Chem.* **2014**, *5*, 6990.
- [20] a) H. T. T. Duong, T. L. U. Nguyen, J. Kumpfmüller, M. H. Stenzel, *Aust. J. Chem.* **2010**, *63*, 1210; b) J. Liu, H. Liu, C. Boyer, V. Bulmus, T. P. Davis, *J. Polym. Sci., Part A: Polym. Chem.* **2009**, *47*, 899.
- [21] V. Ladmiral, G. Mantovani, G. J. Clarkson, S. Cauet, J. L. Irwin, D. M. Haddleton, *J. Am. Chem. Soc.* **2006**, *128*, 4823.
- [22] J. Dai, S. H. Goh, S. Y. Lee, K. S. Siow, *Polym. J.* **1994**, *26*, 905.
- [23] J. Ruokolainen, R. Mäkinen, M. Torkkeli, T. Mäkelä, R. Serimaa, G. t. Brinke, O. Ikkala, *Science* **1998**, *280*, 557.
- [24] S. Valkama, H. Kosonen, J. Ruokolainen, T. Haatainen, M. Torkkeli, R. Serimaa, G. ten Brinke, O. Ikkala, *Nat. Mater.* **2004**, *3*, 872.
- [25] Y. Zhao, K. Thorkelsson, A. J. Mastroianni, T. Schilling, J. M. Luther, B. J. Rancatore, K. Matsunaga, H. Jinnai, Y. Wu, D. Poulsen, J. M. J. Fréchet, A. Paul Alivisatos, T. Xu, *Nat. Mater.* **2009**, *8*, 979.
- [26] I. N. Kurniasih, H. Liang, P. C. Mohr, G. Khot, J. P. Rabe, A. Mohr, *Langmuir* **2015**, *31*, 2639.
- [27] F. Wendler, J. C. Tom, F. H. Schacher, *Polym. Chem.* **2019**, *10*, 5602.
- [28] X.-D. Huang, S. H. Goh, S. Y. Lee, Z. D. Zhao, M. W. Wong, C. H. A. Huan, *Macromolecules* **1999**, *32*, 4327.